CHEMISTRY OF MATERIALS

Communication

pubs.acs.org/cm

Traversing Material Scales: Macroscale LBL-Assembled Nanocomposites with Microscale Inverted Colloidal Crystal Architecture

Christine M. Andres, Mary L. Fox, and Nicholas A. Kotov*

Department of Chemical Engineering, University of Michigan, Ann Arbor, Michigan 48109, USA

Supporting Information

KEYWORDS: *composites, 3D organization, layer-by-layer assembly, hybrid material*

As technological advancements in electronic, biomedical, optical and magnetic applications demand novel functional materials with vastly enhanced and diversified properties, hybrid inorganic−organic nanocomposites have become a fast growing area of materials science research.[1] Nanocomposites demonstrate superior properties to their bulk material counterparts due to the unique characteristics of the individual nanoscale building blocks, and their synergistic interactions with the organic phase. The overall material performance depends on the structure of the interfacial layer between the organic and inorganic components and the three-dimensional (3D) organization of the material across multiple length scales. Development of a systematic approach to investigate the effect of microscale architecture on the macroscale properties of nanocomposites is interesting for numerous reasons. First, the introduction of 3D architecture provides an opportunity to impart unique characteristics to materials such as special deformation patterns,[2] negative Poisson's ratio,[3] negative thermal expansion,[4] controlled biological interactions,[5] and mass transport properties.[6,7] Second, it creates opportunities for new practical applications by allowing unusual *combinations* of properties that previously have not been achieved, as exemplified, for example, by the well-known Ashby diagrams.[8] Third, it aids in bridging the gap between nanoscale materials and macroscale applications, as is currently one of the most significant challenges in material science. Finally, while computational predictions of unique properties of 3D topological structures are quite abundant, actual methods for fabrication of controlled 3D architecture are quite limited and often restricted to multistep adaptations of 2D processes that introduce structural restrictions, are time-consuming, and require expensive hardware.

Most 3D fabrication case studies have been carried out on materials sculpted by photolithography, folding of planar materials, and direct 3D lithography[9−13] or serial alternatives including free-form fabrication,[14] micromachining,[15] and direct-write with colloidal dispersions.[16,17] A lot of success has been achieved in this area aimed predominantly toward applications in medicine and electronics.[3,5,18−20] However, the variety of materials available to these techniques is quite limited, especially with respect to nanocomposites with unique properties that could be very beneficial to a variety of applications.[21−25] In addition, for methods such as 3D direct-writing and 3D lithography that have produced microscale architectures, the transition to macroscale applications is envisioned to be challenging by requiring massively parallel micromanufacturing processes, for example. Considering these technological needs and challenges, a simple and scalable technique to introduce controlled 3D architecture across multiple length scales to novel nanocomposites is quite interesting from both an academic and applied standpoint.

Nanocomposites with distinctive mechanical, electrical, biological, and optical properties[21−25] have been fabricated by the versatile layer by layer (LBL) assembly technique.[26] While the alternating chemical adsorption of nanoscale layers of different high-molecular-weight species (organic or inorganic) provide thermodynamic control over thickness in one direction on the nanoscale,[27] a number of approaches to spatially control LBL materials across multiple scales and dimensions for incorporation into advanced materials have been employed.[25,28] For example, micro- and nanoscale colloidal particles have been coated with LBL nanocomposites and later removed to create 3D hollow capsules for applications in drug delivery, sensing, catalysis, and microreactors.[29,30] On the macroscale, free-standing metal oxide/polymer hybrid membranes with random microscale architecture have been fabricated from cellulose templates.[31,32] While being very attractive for many advanced applications, macroscale examples of LBL *nanocomposites* with microscale structure or any LBL materials with *ordered* microscale structure have not yet been demonstrated. In this study, the samples obtained on a newly developed LBL deposition system (Figure 1A) demonstrate the production of macroscale objects from LBL nanocomposites with millions of repeating structural units based on inverted colloidal crystal (ICC) architectures. This automated system greatly accelerates the process of LBL deposition onto porous substrates with the aid of suction to facilitate solution diffusion and decrease production time.

A systematic approach to the synthesis of hierarchically ordered porous materials has become attractive due to many promising applications in material science including absorption, separation, drug delivery, catalysis, optics, sensing, tissue

Received: October 25, 2011
Revised: November 29, 2011
Published: December 6, 2011

dx.doi.org/10.1021/cm2030069 | *Chem. Mater.* 2012, 24, 9−11

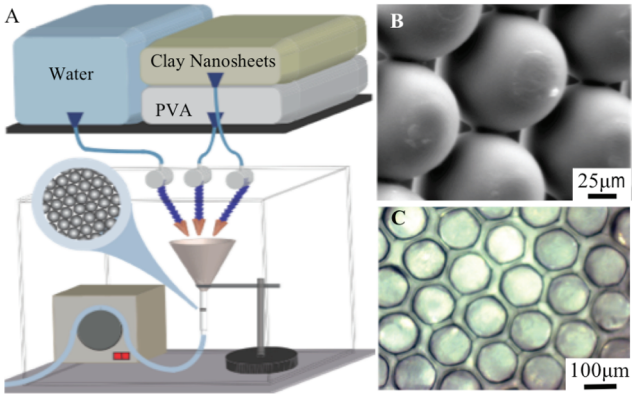

Figure 1. (A) 3D LBL setup used to deliver alternating solutions via solenoid valves through a colloidal crystal template (CCT) secured within silicone tubing and accelerated by a peristaltic pump. (B) SEM image of the annealed polystyrene CCT. Note the necks forming between the beads for pore interconnectivity. (C) Optical microscopy image of the LBL clay nanocomposite on the CCT (B).

engineering, electrodes, and so forth.[33] Colloidal crystal templates (CCT), composed of hexagonally packed arrays of spherical colloidal particles, have served as molds for the synthesis of hierarchically ordered networks with precisely controlled pore size, shape, and order upon infiltration and subsequent removal of the CCT.[33] This technology has been used to pattern and order inorganic nanoscale materials in three dimensions through nanoparticle packing of the CCT voids.[34,35] The random dispersion of nanoparticles within the void leads to low-density packing and often requires annealing to form a mechanically stable 3D structure. Combining LBL deposition and CCT templates allows one to introduce controlled spatial distribution of a nanophase into the bulk of the ICC while retaining the structural control of the microscale architecture and simple scalability to macroscale dimensions.

Uniform polystyrene spheres (diameter ~ 100 μm) were assembled into hexagonally packed arrays via sedimentation and interconnected by annealing at 120 °C to create a CCT as a mold for template LBL (Figure 1B). Interconnectivity of the colloidal spheres provides the structural stability needed for further processing and a template for pore interconnectivity for the final 3D LBL structure. The versatile and simple technique used to create the CCT[36] can be employed to produce a variety of multidimensional shapes when alternative molds or sphere sizes are employed. Anneal times can also be varied to control the diameter of the sphere interconnectivity and later pore interconnectivity as desired.[37]

As successful nanoscale control of clay nanosheets within a polymer matrix has previously been performed two dimensionally with LBL assembly,[22,23] alternative depositions of polyvinyl alcohol (PVA) and clay nanosheets with intermediate rinse-water were used to grow the layered nanocomposite within the void space of the CCT. Scanning electron microscopy (SEM) was used to confirm the presence of the 300 bilayers of nanocomposite on the complex 3D substrate (Figure 1C). While the surfaces of ICC structures have been functionalized by LBL assembly post-production[36,38] and LBL has been used to introduce precursor materials or surface coatings into the voids of CCT,[39,40] to our knowledge, the highly organized and controlled bulk structure of LBL materials have yet to be employed to produce macroscale structures with the controlled ICC microscale architecture.

Upon removal of the polystyrene CCT with tetrahydrofuran, an intact macroscale structure with clear microscale pore definition and interconnectivity is achieved. While suspended in ethanol, optical and confocal microscopy was used to view the microscale architecture and the hierarchical organization of the LBL-assembled nanocomposite (Figure 2A,B). The combination of ICC and LBL assembly provides the systematic assembly of nanomaterials over several discrete length scales. The technique offers a multiscale structure with designed pore size, interconnectivity and organization, wall thickness, and nanoparticle dispersion in the bulk. Controlled spatial arrangement of nanoparticles within the interstitial voids of the CCT and corresponding structure of the ICC is demonstrated for the first time as well as the advancement of freestanding LBL assembled organic–inorganic hybrid nanocomposites to a reproducible 3D macroscale geometry with microscale architecture and the potential to be easily modeled *in silico*.

While 2D LBL films are quite flexible and not very rigid, the interconnected 3D geometry of the ICC structure provides the support needed to allow the structure to exist three-dimensionally with very little material usage. While beneficial for filling the CCT, the combination of the wall flexibility, presence of microscale voids/channels, and hydrophilicity result in structural collapse during simple air drying (Figure 2C). This problem was resolved with freeze-drying to create a self-supporting structure when the strong capillary forces present within the structure during drying were overcome (Figure 2D,E). The 3D controlled pore distribution, size uniformity, and interconnectivity on the microscale are preserved in the dried sample composed of 300 bilayers of PVA and clay nanosheets. It is important to note that, in the case of fairly large clay sheets, the top of the structure becomes completely filled in at some point and prevents further infiltration of the CCT. Obstruction of the smaller channels connecting the interstitial voids during assembly leads to incomplete filling of the voids and insufficient penetration

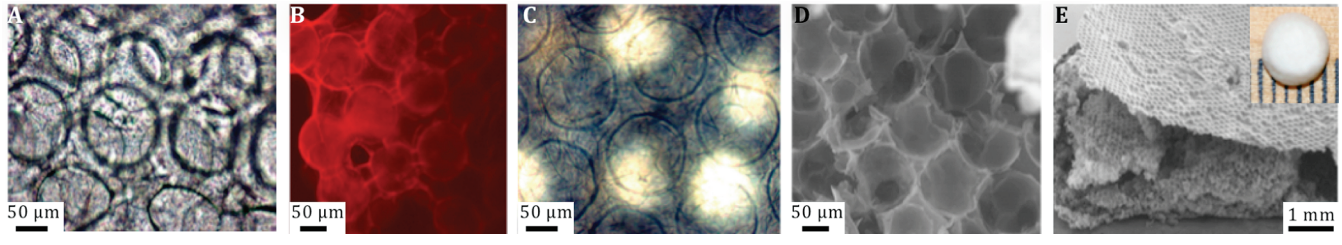

Figure 2. (A) Optical and (B) confocal microscopy images of the microscale architecture of the LBL clay nanocomposite material suspended in ethanol after dissolution of the CCT. (C) Optical images of the microstructure after dried in air and (D,E) SEM images of the freestanding freeze-dried LBL clay nanocomposite structure with an inset showing the macroscale size and shape before cutting in half (tick marks are 1 mm).

dx.doi.org/10.1021/cm2030069 | *Chem. Mater.* 2012, 24, 9–11

throughout all parts of the mold. The technique is limited by mass transport during the assembly of nanosheets and polymers on the complex template. The use of clay nanosheets presents advantages in respect to mechanical properties,[41] catalysis, and drug delivery;[42] however, we expect by taking advantage of the LBL assembly of smaller nanoparticles the mass transport limitation could be overcome to some extent.

The fabrication technique presented allows for complex materials with well-controlled architectures on the macroscale and microscale to be created and integrated with nanoscale organization. Besides the technological promise of such hierarchically organized structures, the fabrication technique presented allows for fundamental study of structure−property relations and the delivery of macroscale nanocomposites by design. Repeatable, controlled spatial arrangement of nanophase materials provides a strategy for tailoring the mechanical, optical, and electrical properties to achieve specific performances. Additionally, the wide variety of materials capable of being assembled using LBL assembly allows for an extensive range of chemical compositions to be employed to otherwise material-limited manufacturing techniques.

The future of 3D LBL for the development of macroscale nanocomposites with microscale architectures for advanced material applications will be dependent on the optimization of the automated fabrication device to provide the fluid mechanics and mass transport conditions for enhanced filling of the CCT, which is suspected to enhance the mechanical properties of the resulting structure, as will be required for many applications.

■ ASSOCIATED CONTENT

Supporting Information

Details of the experimental procedures (PDF). This material is available free of charge via the Internet at http://pubs.acs.org.

■ AUTHOR INFORMATION

Corresponding Author

*E-mail: kotov@umich.edu.

■ ACKNOWLEDGMENTS

The work is mainly supported by AFOSR M4 Project FA9550-08-1-0382 and AFOSR MURI 444286-P061716 and NIH 1R21CA121841-01A2. This material is based upon work partially supported by the Center for Solar and Thermal Energy Conversion, an Energy Frontier Research Center funded by the U.S. Department of Energy Office of Basic Energy Sciences under Award Number #DE-SC0000957. We acknowledge support from NSF under Grant ECS-0601345; EFRI-BSBA 0938019; CBET 0933384; CBET 0932823; CBET 1036672; and a Graduate Research Fellowship. Finally, the authors thank the University of Michigan's EMAL for its assistance with electron microscopy.

■ REFERENCES

(1) Merhari, L. *Hybrid Nanocomposites for Nanotechnology Electronic, Optical, Magnetic and Biomedical Applications*; Springer-Verlag US: Boston, MA, 2009.

(2) Sayle, T. X. T.; Ngoepe, P. E.; Sayle, D. C. *ACS Nano* **2009**, *3* (10), 3308.

(3) Lakes, R. *Science* **1987**, *235* (4792), 1038.

(4) Sigmund, O.; Torquato, S. *J. Mech. Phys. Solids* **1997**, *45* (6), 1037.

(5) Hollister, S. J. *Nat. Mater.* **2005**, *4* (7), 518.

(6) Philippi, P. C.; Souza, H. A. *Int. J. Multiphase Flow* **1995**, *21* (4), 667.

(7) Vrettos, N. A.; Imakoma, H.; Okazaki, M. *Chem. Eng. Process.* **1989**, *26* (3), 237.

(8) Ashby, M. F. *Materials selection in mechanical design*, 4th ed.; Butterworth-Heinemann: Amsterdam, 2011.

(9) Leong, T. G.; Zarafshar, A. M.; Gracias, D. H. *Small* **2010**, *6* (7), 792.

(10) Xu, B.; Arias, F.; Brittain, S.; Zhao, X.; Grzybowski, B.; Torquato, S. *Adv. Mater.* **1999**, *11* (14), 1186.

(11) Campbell, M.; Sharp, D. N.; Harrison, M. T.; Denning, R. G.; Turberfield, A. J. *Nature* **2000**, *404* (6773), 53.

(12) Lin, S. Y.; Fleming, J. G.; Hetherington, D. L.; Smith, B. K.; Biswas, R.; Ho, K. M.; Sigalas, M. M.; Zubrzycki, W.; Kurtz, S. R.; Bur, J. *Nature* **1998**, *394* (6690), 251.

(13) Moon, J. H.; Ford, J.; Yang, S. *Polym. Adv. Technol.* **2006**, *17* (2), 83.

(14) Wendel, B.; Rietzel, D.; Kühnlein, F.; Feulner, R.; Hülder, G.; Schmachtenberg, E. *Macromol. Mater. Eng.* **2008**, *293* (10), 799.

(15) Gattass, R. R.; Mazur, E. *Nat. Photonics* **2008**, *2* (4), 219.

(16) Smay, J.; Gratson, G.; Shepherd, R.; Cesarano, J.; Lewis, J. *Adv. Mater.* **2002**, *14* (18), 1279.

(17) Lewis, J. A. *Adv. Funct. Mater.* **2006**, *16* (17), 2193.

(18) Deubel, M.; Von Freymann, G.; Wegener, M.; Pereira, S.; Busch, K.; Soukoulis, C. M. *Nat. Mater.* **2004**, *3* (7), 444.

(19) Jackman, R. J.; Brittain, S. T.; Adams, A.; Prentiss, M. G.; Whitesides, G. M. *Science* **1998**, *280* (5372), 2089.

(20) Gratson, G. M.; Xu, M. J.; Lewis, J. A. *Nature* **2004**, *428* (6981), 386.

(21) Tang, Z. Y.; Wang, Y.; Podsiadlo, P.; Kotov, N. A. *Adv. Mater.* **2006**, *18* (24), 3203.

(22) Tang, Z. *Nat. Mater.* **2003**, *2* (6), 413.

(23) Podsiadlo, P.; Kaushik, A. K.; Arruda, E. M.; Waas, A. M.; Shim, B. S.; Xu, J. D.; Nandivada, H.; Pumplin, B. G.; Lahann, J.; Ramamoorthy, A.; Kotov, N. A. *Science* **2007**, *318* (5847), 80.

(24) Mamedov, A. A.; Kotov, N. A.; Prato, M.; Guldi, D. M.; Wicksted, J. P.; Hirsch, A. *Nat. Mater.* **2002**, *1* (3), 190.

(25) Hammond, P. T. *Adv. Mater.* **2004**, *16* (15), 1271.

(26) Decher, G. *Science* **1997**, *277* (5330), 1232.

(27) Ostrander, J. W.; Mamedov, A. A.; Kotov, N. A. *J. Am. Chem. Soc.* **2001**, *123* (6), 1101.

(28) Wang, Y.; Angelatos, A. S.; Caruso, F. *Chem. Mater.* **2008**, *20* (3), 848.

(29) De Geest, B. G.; De Koker, S.; Sukhorukov, G. B.; Kreft, O.; Parak, W. J.; Skirtach, A. G.; Demeester, J.; De Smedt, S. C.; Hennink, W. E. *Soft Matter* **2009**, *5* (2), 282.

(30) Caruso, F.; Caruso, R. A.; Mohwald, H. *Science* **1998**, *282* (5391), 1111.

(31) Gu, Y. Q.; Huang, J. G. *J. Mater. Chem.* **2009**, *19* (22), 3764.

(32) Strydom, S. J.; Otto, D. P.; Liebenberg, W.; Lvov, Y. M.; de Villiers, M. M. *Int. J. Pharm.* **2011**, *404* (1−2), 57.

(33) Stein, A.; Li, F.; Denny, N. R. *Chem. Mater.* **2008**, *20* (3), 649.

(34) Vlasov, Y. A.; Yao, N.; Norris, D. J. *Adv. Mater.* **1999**, *11* (2), 165.

(35) Huang, L. M.; Wang, Z. B.; Sun, J. Y.; Miao, L.; Li, Q. Z.; Yan, Y. S.; Zhao, D. Y. *J. Am. Chem. Soc.* **2000**, *122* (14), 3530.

(36) Lee, J.; Shanbhag, S.; Kotov, N. A. *J. Mater. Chem.* **2006**, *16* (35), 3558.

(37) Cuddihy, M. J.; Kotov, N. A. *Tissue Eng., Part A* **2008**, *14* (10), 1639.

(38) Wang, D.; Caruso, F. *Chem. Commun.* **2001**, *5*, 489.

(39) Wang, Y. J.; Caruso, F. *Adv. Funct. Mater.* **2004**, *14* (10), 1012.

(40) Arsenault, A. C.; Halfyard, J.; Wang, Z.; Kitaev, V.; Ozin, G. A.; Manners, I.; Mihi, A.; Míguez, H. *Langmuir* **2004**, *21* (2), 499.

(41) Ma, W.; Otsuka, H.; Takahara, A. *Chem. Commun.* **2011**, *47* (20), 5813.

(42) Lvov, Y. M.; Shchukin, D. G.; Möhwald, H.; Price, R. R. *ACS Nano* **2008**, *2* (5), 814.